

Supernova/Acceleration Probe (SNAP): Summary

ABSTRACT

The Supernova/Acceleration Probe (SNAP) is a mission concept for a 2.0-meter space telescope with up to a one-square-degree field of view. A near one-billion-pixel wide-field imaging system is comprised of 144 large format new technology CCD's sharing a focal plane with 18-36 HgCdTe detectors. Both the imager and a low resolution ($R \sim 100$) spectrograph cover the wavelength range 3500 - 17000 Å. The primary aims are to measure the properties of the accelerating universe and study both the dark energy and the dark matter of the Universe using supernovae and weak gravitational lensing; parallel and Guest Survey science is discussed in the companion paper. SNAP can discover and follow over 2500 Type Ia supernovae every year at redshifts $z = 0.3 - 1.7$. The resulting magnitude-redshift relation can determine the cosmological parameters with high precision: mass density Ω_M to ± 0.02 , vacuum energy density Ω_Λ and curvature Ω_k to ± 0.05 , and the dark energy equation of state w to ± 0.05 and its time variation $w' = dw/dz$ to ± 0.15 . Wide area weak gravitational lensing studies will map the distribution of dark matter in the universe.

1. Primary Science

In the past decade the study of cosmology has taken its first major steps as a precise empirical science, combining concepts and tools from astrophysics and particle physics. The most recent of these results is the startling discovery that the Universe's expansion is apparently accelerating rather than decelerating as expected from ordinary gravity. This implies that the simplest model for the Universe – flat and dominated by matter – appears not to be true, and that our current fundamental physics understanding of particles, forces, and fields is likely to be incomplete.

The clearest evidence for this surprising conclusion comes from the recent super-

nova measurements of changes in the Universe's expansion rate that directly show the acceleration. Figure 1 plots the results of Perlmutter et al. (1999) (see also Riess et al. (1998)) who use a Hubble diagram for 42 SNe with $0.18 < z < 0.83$ to find that for a flat universe $\Omega_M = 0.28 \pm 0.08$ ($\Omega_\Lambda = 1 - \Omega_M$), and constrain the combination $0.8\Omega_M - 0.6\Omega_\Lambda$ to -0.2 ± 0.1 .

This evidence for a negative pressure vacuum energy density is in remarkable concordance with combined galaxy cluster measurements (Bahcall et al. 1999), which find $\Omega_M \approx 0.3$, and current CMB results (Balbi et al. 2000; Lange 2001), which find a flat universe $\Omega_k \approx 0$ (see Fig. 1). Two of these three independent measurements

and standard inflation would have to be in error to make the cosmological constant (or other negative pressure dark energy) unnecessary in the cosmological models.

These measurements indicate the presence of a new, unknown energy component that can cause acceleration, hence having equation of state $w \equiv p/\rho < -1/3$. This might be the cosmological constant. Alternatively, it could be that this dark energy is due to some other primordial field with different dynamical properties, e.g. quintessence. The fundamental importance of a universal vacuum energy has sparked a flurry of activity in theoretical physics. Placing some constraints on possible dark energy models, Perlmutter et al. (1999) and Garnavich et al. (1998a) find that for a flat Universe, the data are consistent with a cosmological-constant equation of state with $0.2 \lesssim \Omega_M \lesssim 0.4$ (Fig. 2), or generally $w < -0.4$ at 95% confidence level. With the use of large scale structure or CMB data the limits push down to $w \leq -0.6$ (Perlmutter, Turner, & White 1999; Garnavich et al. 1998b; Efstathiou 1999).

Connecting Quarks with the Cosmos: Eleven Science ‘Questions for the New Century’, Phase I of the NRC study on the Physics of the Universe, notes “Deciphering the nature of dark matter and dark energy is one of the most important goals in the physics of the universe. The solutions to these problems will cast light not only on the fate of the universe but the very nature of matter, space, and time.”

SNAP will answer this fundamental challenge by constructing a supernova Hubble diagram that will achieve a new level of control over systematic uncertain-

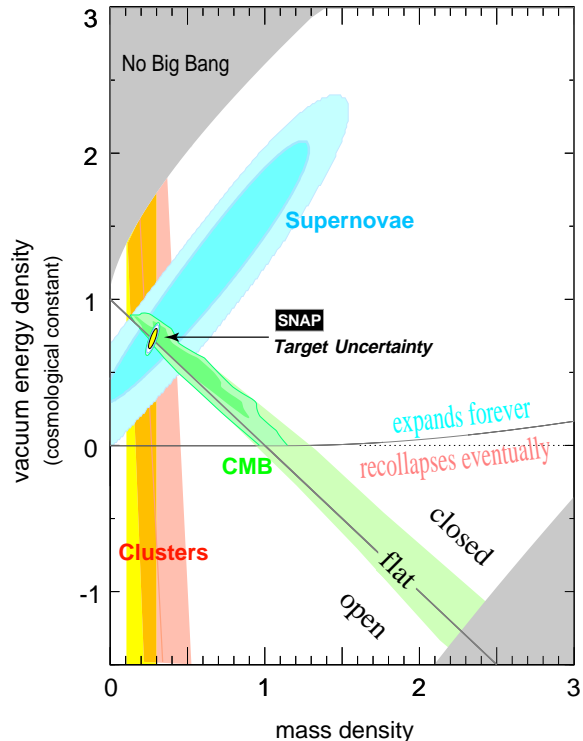


Fig. 1.— Plotted are Ω_M — Ω_Λ confidence regions for current SN (Perlmutter et al. 1999), galaxy cluster, and CMB results. These results rule out a simple flat, [$\Omega_M = 1$, $\Omega_\Lambda = 0$] cosmology; their consistent overlap is a strong indicator for dark energy. Also shown is the expected confidence region from the SNAP satellite for an $\Omega_M = 0.28$ flat Universe.

ties, addressing all of the known and proposed sources of possible error. This would be a landmark fundamental measurement, a clear history of the expansion rate over the past 10 billion years. The precision determination of Ω_M and Ω_Λ would complement planned precision measurements from the CMB and astronomical studies (they would be largely orthogonal in the Ω_M - Ω_Λ plane). The measurement of curvature itself would test the standard

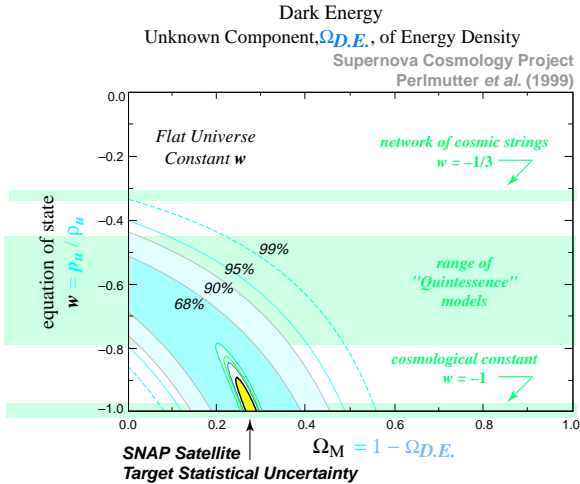


Fig. 2.— Best-fit 68%, 90%, 95%, and 99% confidence regions in the Ω_M - w plane for an additional energy density component, Ω_w , characterized by an equation-of-state $w = p/\rho$. (For Einstein’s cosmological constant, Λ , $w = -1$.) The fit is constrained to a flat cosmology ($\Omega_M + \Omega_w = 1$). Also shown is the expected confidence region allowed by SNAP assuming $w = -1$ and $\Omega_M = 0.28$.

cosmological model, by comparing a measurement at redshift $z \approx 1$ to the CMB curvature measurement at $z \approx 1000$.

SNAP’s science reach then explores the nature of the dark energy, a fundamentally new entity pervading – and dominating – the universe. The simplest measurement here will be the effective pressure to density ratio, $w = p/\rho$, which SNAP can measure to ± 0.05 for a constant- w scenario. However, the practically unconstrained range of dark energy models includes many theories, which can only be differentiated by studying their effect on the universe’s expansion over a wide range

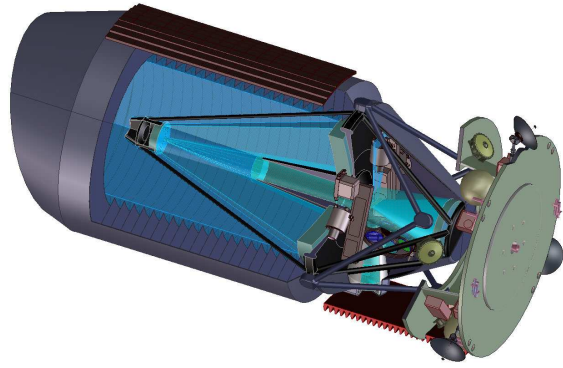


Fig. 3.— A cross-sectional view of the SNAP satellite. The principal assembly components are the telescope, optical bench, instruments, propulsion deck, bus, and thermal shielding.

of redshifts. This is where SNAP’s tight control of systematics and statistical uncertainty at each redshift bin from 0.3 to 1.7 is crucial. Changes in the equation of state, $w' = dw/dz$, are a definitive distinction from a cosmological constant model and will be measurable to ± 0.15 , given independent constraints on Ω_m at the ± 0.04 level (see Table 1). A DOE review states that “SNAP will have a unique ability to measure the variation in w ” – this addresses directly the nature of dark energy.

It is important to note that other cosmological measurements are and will be available, providing complementarity and cross comparison. The simultaneous fit can improve constraints by as much as an order of magnitude – or they may not agree and upset our cosmological understanding. Weak gravitational lensing studies that are an integral part of the SNAP mission can be carried out deeper and clearer than on the ground. They will provide critical information on Ω_M that is key to discerning

TABLE 1
SNAP 1- σ STATISTICAL AND SYSTEMATIC UNCERTAINTIES IN PARAMETER
DETERMINATION.

	σ_{Ω_M}		σ_{Ω_Λ} (or $\sigma_{\Omega_{D.E.}}$)		σ_w		$\sigma_{w'}$	
	stat	sys	stat	sys	stat	sys	stat	sys
$w = -1$	0.02	0.02	0.05	< 0.01
$w = -1$, flat	0.01	0.02
$w = \text{const}$, flat	0.02	0.02	0.05	< 0.01
Ω_M, Ω_k known; $w = \text{const}$	0.02	< 0.01
Ω_M, Ω_k known; $w(z) = w + w' z$	0.08	< 0.01	0.12	0.15

the variation in the equation of state, w' .

As a space experiment SNAP will be able to study supernovae over a much larger range of redshifts than has been possible with the current ground-based measurements – over a wide wavelength range unhindered by the Earth’s atmosphere and with much higher precision and accuracy. Many of these systematics-bounding measurements are only achievable in a space environment with low “sky” noise and a very small point spread function (critical for lensing as well). Unlike other cosmological probes supernova studies have progressed to the point that a detailed catalog of known and possible systematic uncertainties has been compiled – and, more importantly, approaches have been developed to constrain each one.

For example, an approach to the problem of possible supernova evolution uses the rich stream of information that an expanding supernova atmosphere sends us in the form of its spectrum. A series of measurements will be constructed for each supernova that define systematics-

bounding subsets of the Type Ia category. These data (e.g. supernova risetime, early detection to eliminate Malmquist bias, lightcurve peak-to-tail ratio, identification of the Type Ia-defining Si II spectral feature, separation of supernova light from host galaxy light, and identification of host galaxy morphology, etc.) make it possible to study each individual supernova and measure enough of its physical properties to recognize deviations from standard brightness subtypes. Only the change in brightness as a function of the parameters classifying a subtype is needed, not any intrinsic brightness. By matching like to like among the supernova subtypes, we can construct independent Hubble diagrams for each which when compared test systematic uncertainties at the targeted level of 0.02 magnitudes.

Addressing these systematic concerns requires a major leap forward in the measurement techniques. While the thorough study of Type Ia supernovae drives the design of SNAP, described in the next section, the resulting instrument will have

broad capabilities that will be desirable for other astrophysical observations. In particular it is also near optimal for weak gravitational lensing studies. Additionally, SNAP’s primary dataset will survey an area of sky almost 10000 times larger than the Hubble Deep Field and two magnitudes deeper. The rich range of science that can result from this and from SNAP Guest Survey programs is discussed briefly in the companion paper to this description.

2. Mission Design

The baseline proposed satellite experiment is composed of a simple, dedicated combination of a 2.0-meter telescope three-mirror-anastigmat with a nearly 1-square-degree optical-NIR imager and a low resolution ($R \sim 100$) spectrograph, both sensitive in the wavelength range 3500 – 17000 Å (see Figure 3). The mirror aperture is about as small as it can be before spectroscopy at the requisite resolution becomes instrument-noise limited. The imager’s wide field of view enables multiplexing observations for simultaneous supernovae discovery and follow-up photometry. The spectrograph covers for $0 < z < 1.7$ the supernova restframe optical range, including the Si II 6150 Å feature that both identifies SNe Ia and provides a key measurement of the explosion physics to probe the progenitor state. At $z = 1.7$, for example, it spans 1300-6300Å, also allowing observing in the restframe near UV.

Our baseline configuration is a three-mirror anastigmat in which the tertiary mirror re-images an intermediate Cassegrain focus onto the detector plane. This optical train achieves a large flat focal surface with acceptable image quality without the

use of refractive correctors. As with other anastigmats, it is free from spherical aberration, coma and astigmatism. There are further practical advantages to this configuration: baffling against stray light is simpler and the focal plane is more accessible. It possesses two beam waists: one at the Cassegrain focus near the primary mirror, and a second midway between the tertiary mirror and the detector plane. This second waist is small, and is an effective location for our CCD shutter. This optic delivers a root-mean-square image blur of 3 microns (0.03”) over a working field of view extending out to 42’ off the geometrical axis; the resulting point spread function is diffraction limited and stable. An interesting feature of our design is the placement of a pickoff mirror at the second beam waist, which obscures the central part of the field, thus giving the SNAP focal plane an annular field-of-view.

The wide-field imager employs a mosaic of new technology n-type high-resistivity CCD’s (Holland et al. 1999; Stover et al. 1999; Groom et al. 2000) that have high quantum efficiency for wavelengths between 0.3 and 1.0 microns. Each of the $3k \times 3k$ CCD’s have $10.5 \mu\text{m}$ pixels which give 0.1” per pixel with readout noise of $4e^-$ and dark current of $0.08e^- \text{min}^{-1} \text{pixel}^{-1}$. For the infrared it uses an array of 18-36 HgCdTe detectors similar to those for the Hubble Space Telescope Wide Field Camera 3; we will use commercially available $2k \times 2k$, $1.7 \mu\text{m}$ cutoff devices with $18 \mu\text{m}$ pixels (Johnson et al. 2000).

Fixed filters are placed on each detector, covering 9 wavelength bands between 0.35 and 1.7 microns, arranged such that each piece of sky will be observed in each

filter with a shift and stare mode of operation (Figure 4). The relative areas of each filter are proportional to the exposure times required for the supernova program. The brighter low-redshift supernovae will require short blue exposures (in the observer frame) whereas distant supernovae will be observed with deep red integrations. Within the constraints of CCD and HgCdTe packaging, the NIR filters will cover more area than their optical counterparts.

The wide field of view of the imager allows simultaneous batch discovery and photometry of ~ 2500 SNe/year with the proposed accuracy, and even higher numbers of more distant, less precisely measured supernovae. Some 5000 quasars to $M_B = -23$, 10^5 AGNs to $M_B = -16$, possibly 30000 lensed images, and a plethora of other objects should be found within the baseline area almost 10000 times that of the Hubble Deep Field and twice as deep.

The spectrograph employs an “integral field unit” (IFU) to obtain an effective image of a $2''$ by $2''$ field, split into approximately $0.1''$ by $2''$ regions that are each individually dispersed to obtain a flux at each position and wavelength (sometimes called a three-dimensional “data cube”). A schematic of the IFU concept is given in Figure 5. A prism provides a high-throughput dispersive element that makes possible observations of $z = 1.7$ supernovae, at Vega magnitude 23.86 at $\lambda = 1.6\mu\text{m}$, with a 2-m aperture telescope. The broad supernova features accommodate the low dispersion and the decreasing resolution for increasing wavelengths naturally follows the feature broadening at higher redshifts. The detector is a sin-

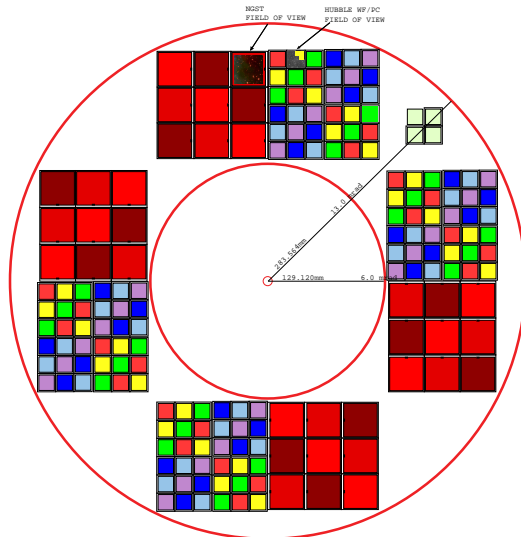


Fig. 4.— The CCD mosaic camera is tiled with 144 $3\text{k} \times 3\text{k}$ high-resistivity CCD’s and 36 HgCdTe detectors covering one square degree. The annular shape is necessary in a simple three-mirror anastigmat telescope design. The small devices at upper right are used in guiding.

gle thinned HgCdTe chip (whose technology is in development for the NGST) that will provide high quantum efficiency from $0.4-1.7\mu\text{m}$. In operation, the integral field unit will allow simultaneous spectroscopy of a supernova target and its surrounding galactic environment; the $2''$ by $2''$ field of view also removes any requirement for precise positioning of a supernova target in a traditional spectrograph slit, simplifies eventual reference galaxy subtraction, and allows us to obtain spectrophotometry.

This instrumentation will be used with a simple, predetermined observing strategy designed to repeatedly monitor a dozen square degrees near the north and south ecliptic poles. Every field will be visited every ~ 4 days with single scans reaching

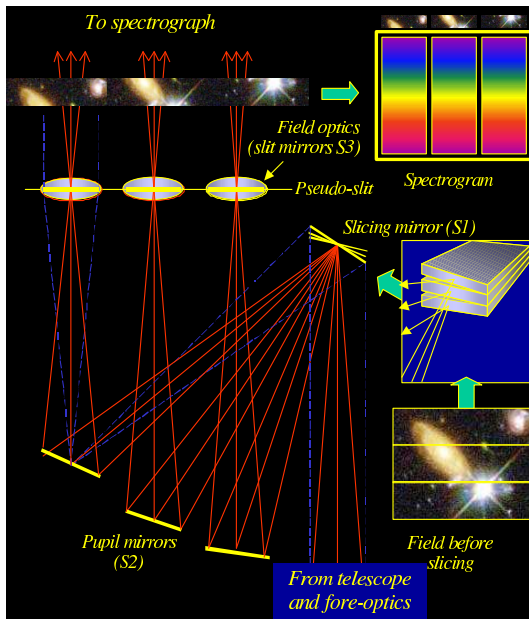


Fig. 5.— A schematic of how an IFU works. A $2''$ by $2''$ field containing the supernova and galaxy, shown in the bottom right, is split into strips by a slicing mirror. Separate pupil mirrors align and direct the strips down a pseudo-slit. The light is then sent to the spectrograph, giving a spectrum for a two-dimensional grid of the image.

$m_{AB} = 28.8$; coadded images are planned to achieve $m_{AB} = 31.6$. Spectroscopy of supernova targets is triggered after discovery; simultaneous photometry and spectroscopy will be possible. However, separate time will be allocated to the targeted spectroscopic program as the random positions of the supernovae on the field will not ensure uniform imaging coverage.

This prearranged photometric observing program is designed to provide a uniform, standardized, calibrated dataset for each supernova, allowing for the first time comprehensive comparisons across com-

plete sets of supernovae. Host galaxy luminosity, colors, morphology, and type are also obtained, and the observing requirements also yield data ideal as survey images. Full data downlink allows archiving and analysis for a variety of science without “biased” preprocessing; some areas of astrophysical study that might take advantage of the data are discussed in the companion paper.

REFERENCES

- Bahcall, N. A., et al. 1999, *Science*, 284, 1481
- Balbi, A., et al. 2000, *ApJ*, 545, L1
- Efstathiou, G. 1999, *MNRAS*, 310, 842
- Garnavich, P., et al. 1998a, *ApJ*, 493, L53
- Garnavich, P., et al. 1998b, *ApJ*, 509, 74
- Groom, D., et al. 2000, *NIM*, A442, 216
- Holland, S., et al. 1999. In *Proc. 1999 IEEE Workshop on Charge-Coupled Devices and Advanced Image Sensors*
- Johnson, J., et al. 2000. In *Space Astrophysics Detectors and Detector Technologies*
- Lange, A., et al. 2001, *PRD*, 63, 042001
- Perlmutter, S., et al. 1999, *ApJ*, 517, 565
- Perlmutter, S., Turner, M. S., & White, M. 1999, *Physical Review Letters*, 83, 670
- Riess, A., et al. 1998, *AJ*, 116, 1009
- Stover, R., et al. 1999. In *Proc. 4th ESO Workshop on Optical Detectors for Astronomy*